EFFICIENT SOLUTION OF LARGE MOMENTS PROBLEMS:

WIRE GRID MODELING CRITERIA AND CONVERSION TO SURFACE CURRENTS

Thomas R. Ferguson

Robert J. Balestri

This work was supported by the Rome Air Development Center Contract F30602-74-C-0182. Portions of this paper were presented at the 1976 EMP Interaction and Coupling Analysis and Validation Seminar, USAF Academy, July 20-22, and at the IEEE 1976 International Symposium on Electromagnetic Compatibility, Washington, D.C., July 13-15.

Thomas Ferguson is currently with the AFWL, Kirtland AFB, NM. Robert Balestri is currently with Booz•Allen & Hamilton, 4330 East West Highway, Bethesda, MD 20814.

ABSTRACT

A banded matrix iterative solution method for linear simultaneous equations arising from thin wire moments problems has been applied to a variety of problems of intermediate electrical size with the number of unknowns ranging up to 1000. Using a convergence criterion of 1 percent, solution efficiencies varied from 2.5 for short, fat objects up to 35 for long, thin objects. Application of the method requires some expertise. Approximate guidelines for wire grid modeling of surfaces have been developed for the moments formalism used. A new method for computing surface currents from grid currents is discussed.

AUTHOR'S NOTE

This article was originally submitted to IEEE-AP in 1977 for publication. As received, it was turned down due to emphases on the computational aspects. The computational techniques have been incorporated into the GEMACS computer code.

Since this work, there has been much activity related to modeling large structures. While GEMACS is not capable of exploiting computer architecture to reduce computational cost, this work clearly demonstrates that large problems can be solved efficiently using peripheral processors and asynchronous input/output operations.

A brief addendum is provided which to some degree substantiates the rather surprising modeling guidelines of length to radius ratios of 5 for square grid representations of solid surfaces.

This paper is being printed in the ACES Journal and Newsletter in order that the results may be available to individuals to whom the computational and modeling aspects of wire grid or patch models are more significant.

1. INTRODUCTION

The BMI (banded matrix iterative) solution method was developed to reduce the cost of solving the linear simultaneous equations arising from the thin wire method of moments formalism. The results have been reported in detail.[1] A summary of the theory and results for small problems has been published.[2] This paper is a summary of the study of intermediate to large size problems (100 to 1000 unknowns). The majority of the problems investigated are wire grid models of objects with surface areas ranging up to 10 square wavelengths. Intermediate sized problems of this type were investigated to establish wire grid modeling criteria.[1d] These criteria were used in larger problems to investigate the solution efficiency of the BMI method.[1e] The reported formula for converting grid currents to surface currents was established in retrospect.

2. THEORY

The equations to be solved are written

$$AX = b, \tag{1}$$

where A is a full complex nonsymmetric N x N matrix usually called the impedance matrix, X is a column vector of N unknowns related to the coefficients in the current expansion, and b is the excitation column vector. The least expensive general method for solving these equations is by triangular decomposition of A using Gaussian elimination, which requires about $N^3/3$ complex multiplicative operations (MOs). An approximate solution with an accuracy of about 1 percent can be obtained at less expense by making use of knowledge about the elements of A. The wire segment self impedances (principal diagonal elements of A) are always large. The relative size of segment interactions (off-diagonal elements) decreases with increasing separation. Near neighbor interactions can be as large as the self terms.

Suppose the wire segments are numbered in the following manner. The object model is sliced into parallel sections across the most narrow dimension. All wire segments in an extreme slice are numbered first. All

segments are then numbered in the adjacent slice, and the process is repeated to the opposite extremity of the object. The slices are kept thin so that numbering proceeds across the object within a slice. As a result, the difference in segment numbers between segments in neighboring slices is always much less then N, the total number of segments. For problems of significant electrical size, the large off-diagonal matrix elements are the interactions between segments with separations much less than the object length. These matrix elements can be grouped within a small bandwidth about the principal diagonal using this numbering scheme.

The BMI solution method takes advantage of these characteristics by partitioning the matrix as

$$A = L + B + U, \tag{2}$$

where B is a banded matrix of equal upper and lower bandwidths M, and L and U are the strictly lower and upper triangular matrices below and above B in A. Then (1) can be written as

$$BX = b - (L + U)X. \tag{3}$$

The banded matrix is decomposed into a product of a banded lower triangulation matrix B_L and a banded upper matrix B_U by pivoting on the principal diagonal elements. An iterative sequence is then defined by the solutions of

$$B_L B_U X_{i+1} = b - (L + U)X_i. \tag{4}$$

Forward elimination and back substitution are required for each iteration. Assuming that the decomposition of B does not lead to large rounding errors, the sequence $\{X_i\}$ will converge to a solution of (1) if the spectral radius of $B^{-1}(L + U)$ is less than one. Pivoting on the principal diagonal elements theoretically could lead to large rounding errors, especially in ill-conditioned problems. Monitoring of the pivot ratio and comparisons to solutions of canonical problems have provided confidence in this method when used on computers with high precision.

In terms of MOs, the cost of decomposing B is $NM^2 - 2M^3/3$. The cost of each iteration is N^2. Assuming K iterations are required to reach the criterion for convergence, the solution efficiency of the BMI method relative to triangular decomposition of the full matrix is

$$g = N^3\left[3(NM^2 - \frac{2M^3}{3} + KN^2)\right]^{-1}. \quad (5)$$

Termination of the iteration is achieved by imposing a numerical criterion on some measure of convergence. In the early study of small problems, the exact solution x_e was available for comparison. The RE (relative-error) at the j-th iteration was defined by

$$RE_j = \left[\frac{(x_j - x_e)^\dagger(x_j - x_e)}{x_e^\dagger x_e}\right]^{1/2} \quad (6)$$

where (†) denotes the complex conjugate transpose. Because the exact solution is normally not known, some alternative measure is required. One candidate is the BCRE (boundary condition relative error) defined by

$$BCRE_j = \left[\frac{(AX_j - b)^\dagger(AX_j - b)}{b^\dagger b}\right]^{1/2} \quad (7)$$

Unfortunately, the ratio of the RE to the BCRE is bounded between the condition number of A and its reciprocal. This number can be computed at a cost of about N MOs at each iteration, however, and provides useful information about convergence. In particular, an increase in the BCRE has always been found to be a forecast of divergence.

An adequate measure of convergence is the IRE (iterative relative error) defined by

$$IRE_j = \left[\frac{(x_j - x_{j-1})^\dagger(x_j - x_{j-1})}{x_j^\dagger x_j}\right]^{1/2}. \quad (8)$$

For cases of rapid convergence, the sequence of values of both the RE and the IRE can be approximated by an exponential function.[1c] As a result, the value of the IRE at the next iteration can be predicted as

$$IREj+1 \simeq \frac{IRE_j^2}{IRE_{j-1}}. \quad (9)$$

This quantity is called the PRE (predicted relative error). The iteration for large problems was terminated when the PRE was less than 1 percent.

In all calculations, the starting value for x_0 was zero. Once B is decomposed, the cost in MOs for obtaining x_1 is less than N^2 because the operation $(L + U)x_0$ need not be performed. Experience shows that x_1 is a reasonable approximation to the solution in all cases of rapid convergence.

Hence no physical arguments or complicated problem-dependent calculations are required to start the iteration.

If the spectral radius of B^{-1} (L + U) is greater than 1, the sequence $\{x_1\}$ must eventually diverge. However, the sequence may initially converge and then diverge. This behavior is called pseudoconvergence. It has been observed in this study, and the best solution obtained may be of useful accuracy.

3. COMPUTER PROGRAM

The computer program used to investigate the capabilities and limitations of the BMI solution technique for large problems was a modified version of the Antenna Modeling Program.[3] This program is based on the Pocklington integral equation, with pulse plus sine plus cosine expansion functions, point matching, and a charge redistribution scheme at multiple wire junctions that accounts for differing segment lengths. The BMI solution method was incorporated using machine dependent programming techniques peculiar to the CDC computers (flip-flopping of storage areas and simultaneous buffering of data) to reduce costs and turnaround times. Different sections of code were used in the solution process depending on N, M, and a core size allocation parameter to take advantage of cases where A, B, B_L, B_U, or L + U fit entirely in core. This procedure does not affect the computer CP (central processor) time, which depends only in the number of MOs, but reduces the peripheral processor costs for problems of moderate size. Other portions of the program were not optimized, and segmentation was not used to further reduce core requirements. This program will not be disseminated. However, a general modeling program that includes an ANSI FORTRAN version of the BMI solution technique may be available.[4]

4. RESULTS FOR LARGE PROBLEMS

For the segment numbering scheme used, a bandwidth M corresponds to a distance R_M within which all interactions are kept in the banded matrix. During the research phase on small problems, each problem was investigated at several bandwidths to determine the value of M

for peak efficiency using a convergence criterion of 1 percent. The resulting guideline was that R_M should be about 1/7 of the object length. Cost limitations in the study of large problems prohibited varying the bandwidth for each problem. Calendar restrictions together with early convergence difficulties for models of spheres resulted in conservative choices of M for some large problems.

Eleven example problems are briefly described below and in Table 1. Geometric symmetries in these problems were not used to reduce solution costs.

(1) One straight wire, $L/\lambda = 100$.

(2) Four parallel wires, $L/\lambda = 25$.

(3) 10 by 10 array of half wavelength dipoles.

(4) Rectangular plate grid, 2.77 by 3.18 λ.

(5) Rectangular plate grid, 3.0 by 0.637 λ.

(6) Square plate grid, 2.0 by 2.0 λ.

(7) Parabolic cylinder reflector grid with array feed, 2.0 by 2.0 λ.

(8) Cylindrical grid, $L/\lambda = 3.0$, $ka = 1$.

(9) Cylindrical grid, $L/\lambda = 2.8$, $ka = 3.4$.

(10) Cylindrical grid, $L/\lambda = 2.8$, $ka = 3.4$, 24 wires.

(11) Gridded cylinder with axial stubs, $L/\lambda = 2.0$, $ka = 2.1$.

TABLE 1. Efficiency of Solution for Example Large Problems

PROBLEM NUMBER	N	M	K	g
1	1000	150	3	14.3
2	1000	60	6	35.3
3	500	70	1	16.9
4	963	236	3	6.2
5	396	65	4	9.8
6	544	132	2	6.3
7	860	120	1	17.7
8	392	64	3	10.6
9	984	336	9	3.4
10	480	168	11	2.9
11	822	240	7	4.3

These examples include both antennas and scatterers. The above-mentioned guideline for choice of M was used in examples 1,3,5,7, and 8. Convergence was rapid for these problems and the average efficiency was about 14. For example 2, a relatively small bandwidth resulted in high efficiency. Although this result could be problem dependent, the BMI solution method may prove to be more efficient than expected for long, thin objects. For examples 4 and 6, conservative choices for M resulted in rapid convergence. Higher efficiencies would probably be found by using the guideline for these examples. Good efficiencies were obtained for all objects with planar or near-planar geometries. Results for some of these examples using other lengths or wavelengths were comparable, but are not shown in Table 1.

To further exhibit the iteration characteristics for problems with rapid convergence, example 4 is described in greater detail. The grid mesh is square. There are 23 wire segments along one edge and 20 along the other. Numbering is along one edge, then along the adjacent segments perpendicular to the edge, then along the segments parallel to the edge, etc. The excitation is a plane wave with E-polarization and a 45° angle of incidence. The convergence data are shown in Table 2. The efficiency is computed at each iteration from (5) with K as the current number of iterations. As is evident, most of the solution time for this example was spent in decomposing B, and the rapid convergence points to better efficiency at smaller M. The PRE is a fair predictor of the IRE at the next iteration, which is characteristic of cases with rapid convergence. Note that the BCRE is about 1/5 of the IRE at each iteration, which shows that the BCRE is not an adequate measure of convergence. (The pivot ratio for decomposing B was only 53 for this example, indicating that the small values of the BCRE are not due to an ill-conditioned problem.)

TABLE 2. Convergence Data for Example 4; N=963, M=236

ITERATION	EFFICIENCY	BCRE	IRE	PRE
1	6.6	16.9	100.0	—
2	6.5	4.0	19.1	3.6
3	6.4	1.1	4.9	1.3
4	6.2		1.5	.4

The efficiency of the BMI solution method is considerably lower for short, fat objects. The performance for spheres will be discussed later. For a cylinder with length and circumference approximately equal, the guideline for M generally results in divergence or pseudoconvergence. Larger bandwidths yield convergence as shown by examples 9-11, but with lower efficiencies than for planar or long objects. Example 9 exhibits several details of interest. The cylindrical grid has 24 wire segments in a circumference and 20 along a length. Numbering is helix-like, which is a special choice of numbering within each slice across the cylinder. The guideline for M suggests a value of about 144 for this problem. Actual values used were 336, as shown in Table 1, and 195. For a plane wave excitation with E-polarization, the convergence data are shown in Table 3 at a bandwidth of 336. Note again that the BCRE is not a reliable measure of convergence. The PRE is an excellent predictor of the IRE at the next iteration in this example.

TABLE 3. Convergence Data for Example 9; N=984, M=336

ITERATION	EFFICIENCY	BCRE	IRE	PRE
1	3.7	11.93	100.00	—
2	3.7	4.62	45.81	20.98
3	3.6	2.66	20.84	9.48
4	3.6	1.76	13.54	8.80
5	3.5	1.20	9.30	6.39
6	3.5	.81	6.29	4.25
7	3.5	.55	4.30	2.95
8	3.4	.38	2.93	1.99
9	3.4	.26	2.00	1.37
10	3.4		1.36	.93

At a bandwidth of 195, example 9 was studied for E-polarization, H-polarization, and also for an annular gap voltage impressed on longitudinal segments at one cross section of the cylinder. For E-polarization, pseudoconvergence occurred. The best solution was at the fourth or fifth iteration, with an IRE of 26 percent and a BCRE of 6 percent. Compared to the solution obtained at a bandwidth of 336, this solution showed differences ranging up to 30 percent. (Far fields computed from this solution agreed with those from the accurate solution to within about 3

percent.) For H-polarization, the solution diverged after the first iteration. For the gap excitation, pseudoconvergence occurred. The best solution was obtained at the fifth or sixth iteration, with an IRE of 8 percent and a BCRE of 3 percent. These results emphasize the following characteristics of the iterative process. Whether the sequence converges depends on the spectral radius of B^{-1} (L + U) and not on the excitation. The number of iterations required for convergence depends on the spectral radius, the excitation, the starting point, and the convergence criterion.

Several wire grid models of spheres were investigated. Each model was constructed with a finite degree of rotational symmetry. The models generally had wire segments along lines of latitude or longitude, with occasional tapering at moderate latitudes to prevent extreme differences in segment length at junctions near the poles. Solutions were sought with the BMI method without making use of symmetries. Solutions were obtained with the use of symmetries for comparisons in some cases. In the iterative method, segment numbering spirals outward from one pole to helix-like numbering at the equator, and then spirals inward at the other pole.

For a sphere with ka equal to 4.7, a model using 996 segments was used. The excitation was a plane wave, incident normal to the polar axis. The wave had E (case 1) or H (case 2) lying in the equatorial plane. In the first case, pseudoconvergence occurred at bandwidths of 220 and 360. The best solutions obtained were poor. In the second case, at a bandwidth of 220, 33 iterations reduced the IRE to 2.7 percent and the BCRE to 2 percent. Termination was due to an independently set default. No sign of divergence was present. The distribution of current on wires normal to the H plane at the equator was in full agreement with known surface currents. Because pseudoconvergence occurred at a bandwidth of 220 for E-polarization, it must also eventually occur for H-polarization. This example shows that even a fairly small convergence criterion could be satisfied in an iterative sequence eventually destined for divergence.

It is possible that interior mode contributions affect the iterative solution for wire grid models of fat objects. Little is known about such modes. For the spherical cavity, the mode of lowest frequency occurs at ka equal to 2.744. A grid model for this sphere with 552 segments was

subjected to a plane wave excitation. With M equal to 192, pseudoconvergence occurred. The IRE and BCRE were reduced to less than 20 percent at the sixth iteration. The corresponding current distribution and resulting scattering cross section showed fair agreement with known behavior for the sphere external problem.

Additional studies of short, fat objects will be required to establish adequate guidelines for choice of M.

5. COMPUTER COSTS

All of the example problems were run on a CDC 6600 computer. For those examples resulting in convergence, the CP times required for solution are plotted in Figure 1 versus the number of MOs. The CP time is almost entirely due to performing the multiplicative operations, as expected. Time requirements on other machines may be approximated by comparing times required for one multiplication.

The PP (peripheral processor) times for full program execution are plotted in Figure 2 versus the number of MOs. Almost all of the PP time is used during the decomposition of B. The PP time required for performing iterations is quite small. The one point in Figure 2 well below the line is for the sphere problem with 33 iterations mentioned earlier. The large value for K raises the number of MOs considerably without much effect on the PP time. The PP time is dependent on the machine and the operating system, and on the amount of fast access core available for matrix operations. The latter factor determines whether all of A, B, B_L, B_U, or L + U can reside entirely in core. The most significant savings in PP time occur when B will reside in core, which requires about N(2M+1) complex words of storage. None of the large problems satisfied this requirement. Projections of PP time for other computers would be difficult. If M<<N, the PP time for the BMI solution method should be far less than for full decomposition of A. No numerical comparisons were available. The dollar cost for computing was dominated by the PP time.

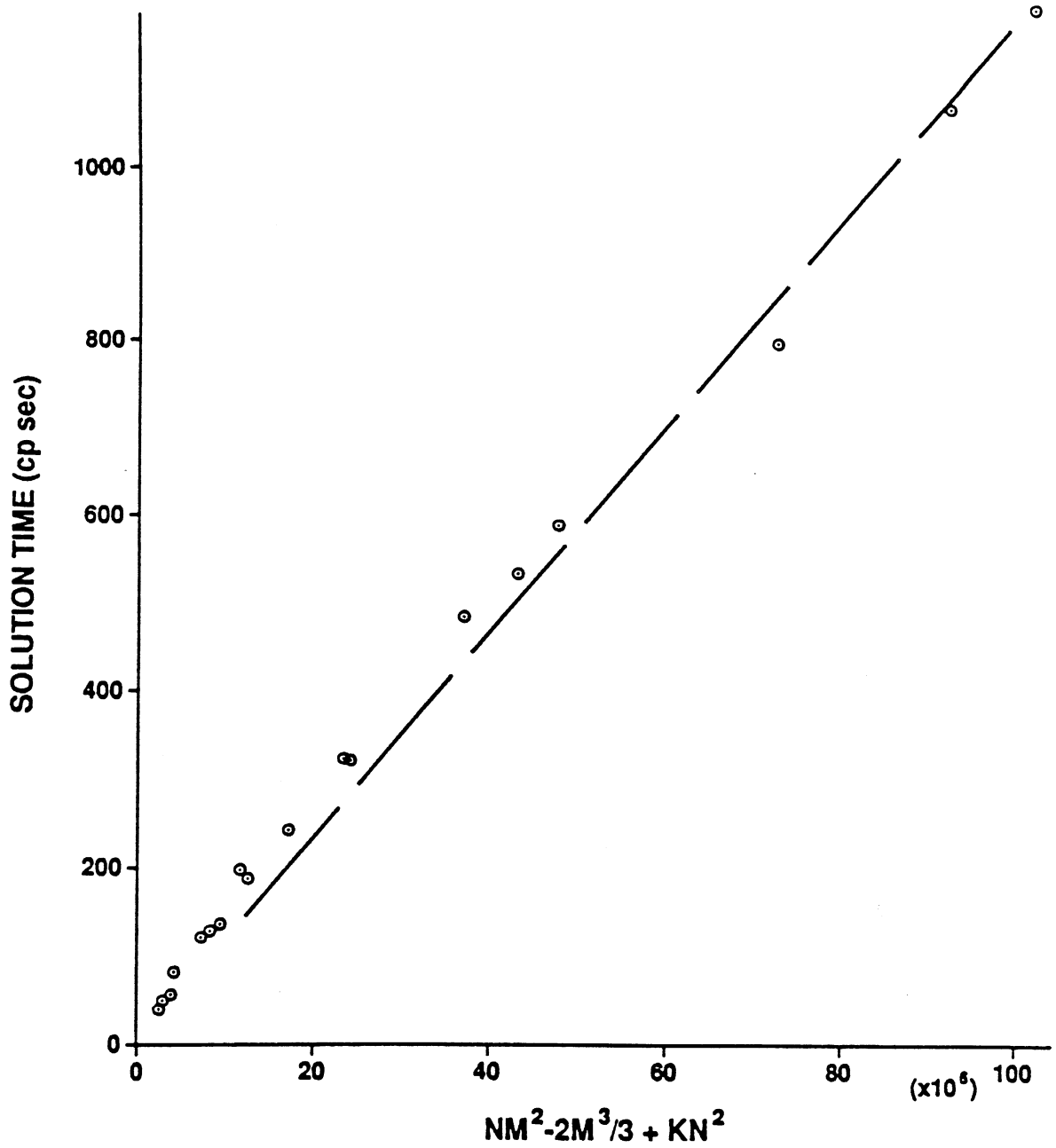

Figure 1. Equation Solution Time Versus Number of Complex Multiplicative Operations

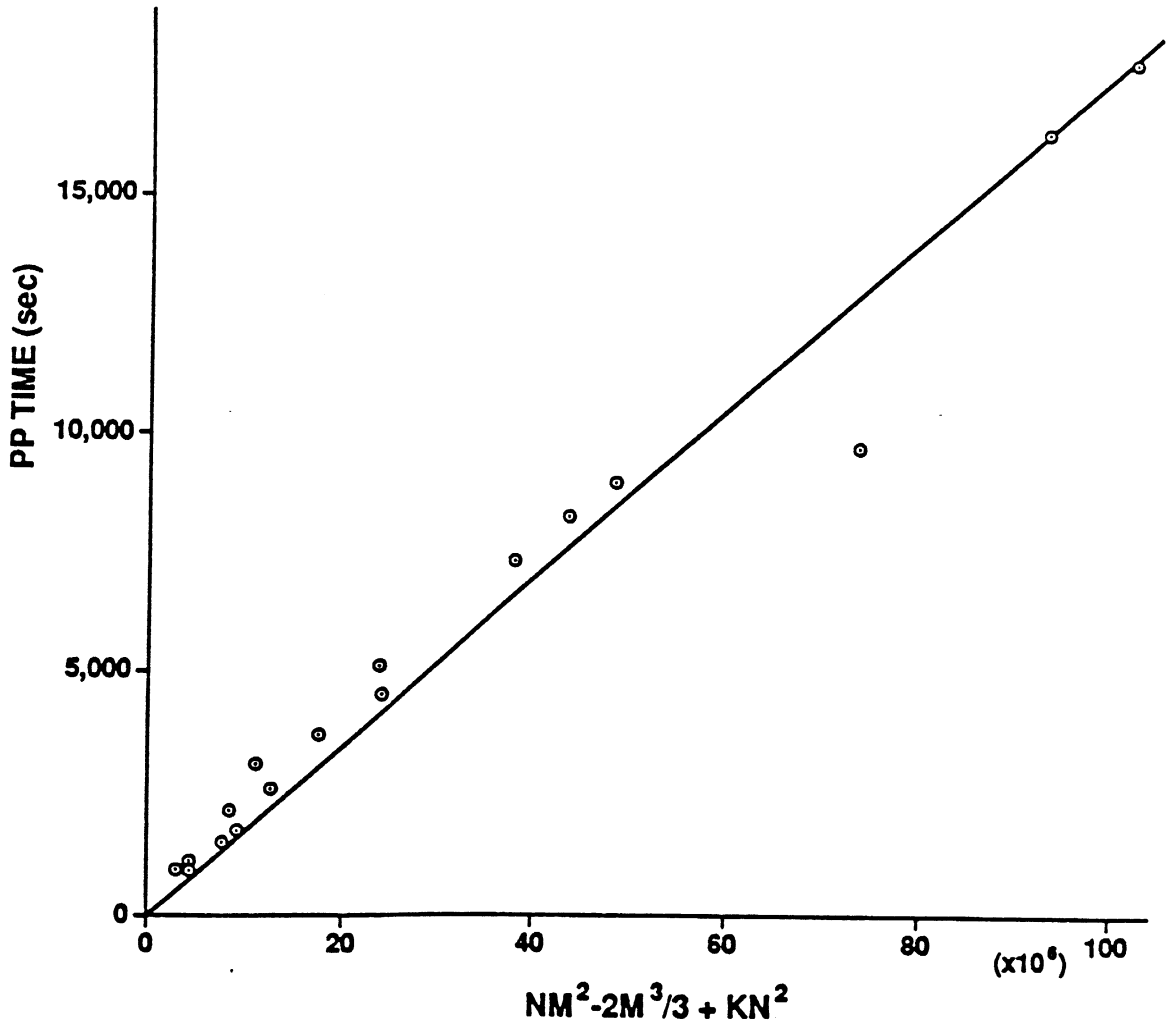

Figure 2. Peripheral Processor Time Versus Number of Multiplicative Operations

6. SURFACE MODELING WITH GRIDS

Early experience with the BMI solution method showed that the convergence properties for wire grid models of conducting surfaces should be based on models that are known to adequately represent the surfaces. Hence a limited modeling study was undertaken. Several objects of moderate size and rotational symmetry were modeled by wire grids with finite degrees of rotational symmetry. Symmetry was used in the solution process to reduce costs.[1d]

Wire grid modeling guidelines are not well defined in the literature. Mesh circumferences must be appreciably less than a wavelength to prevent mesh loop resonance phenomena. The maximum segment length depends on the details of the moments formalism in use, but must be restricted to about one-fifth of a wavelength even for single straight wire problems solved with sophisticated expansion functions. One guideline for the wire radius suggests that the wire surface area be about equal to the area of the modeled surface. Thinner wires have been used. For models with varying mesh shape and size, most studies have used the same wire radius for all segments. This practice was followed here.

No method for accurate conversion of wire grid currents to equivalent surface currents was available during this study. As a consequence. radiation patterns and bistatic scattering cross sections available from the literature for canonical objects were used for comparison to model results. These attributes are not as sensitive as current distributions for comparison purposes. After a conversion method was developed, current comparisons were made in a few cases.

Far field calculations from sphere models were compared to graphed results for radiation patterns of spherical antennas[5] and to bistatic scattering cross sections.[6] The models used wire segments along lines of latitude and longitude, yielding nearly rectangular mesh shapes at the equator.

For a spherical antenna with an equatorial gap and ka equal to 2, the power radiation pattern is shown in Figure 3 as a solid line. The other lines

were computed from the model, with the average ratio of segment length to wire radius at the equator denoted by d. Good agreement was obtained for ka equal to 3. Agreement deteriorated rapidly for ka equal to 4 and 5. Corresponding mesh circumference for the larger mesh area near the equator were 0.35, 0.52, 0.70, and 0.87 wavelengths respectively.

For plane wave scattering by a sphere, the bistatic scattering cross section in the E plane for ka equal to 2.3 is shown by the line in Figure 4. The points were computed from the model. Reasonable values were obtained for d equal to 5. Wire radii were fixed at this value and the frequency was varied. Good agreement was found at lower frequencies. At ka equal to 4.7, corresponding to mesh circumferences of about one wavelength, cross section errors of a factor of 2 were found.

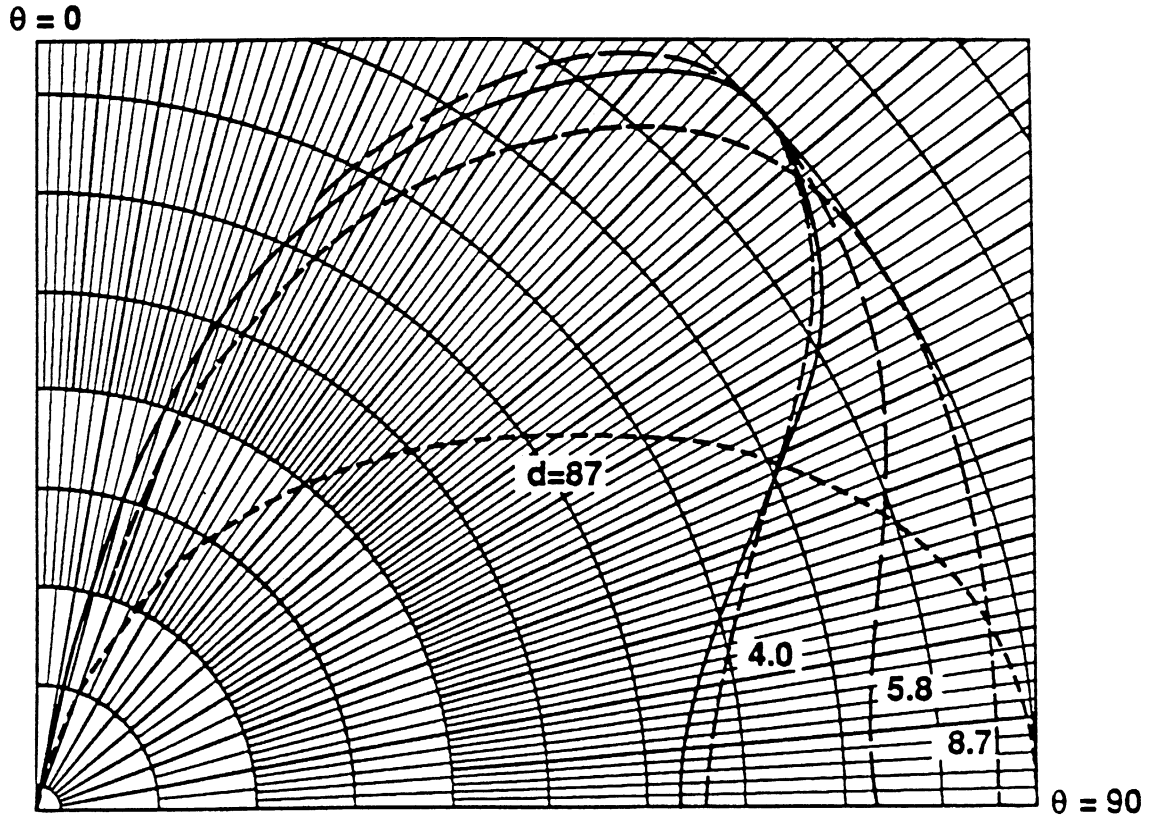

Figure 3. Power Radiation Pattern of a Sphere Excited Across an Annular Gap at the Equator, ka=2. (Solid Line After [5], Others from Model.)

Guidelines suggested by these comparisons are that the largest mesh circumference should not greatly exceed one half wavelength and the ratio of segment length to wire radius in regions of square mesh should be about five. Models of other objects (disk, toroid, cylinder, cone-sphere, etc.) were constructed using these approximate guidelines. Consistently good agreement with other theoretical results were obtained.[1d,e]

The guideline suggests a relatively fat wire for grid models in view of the thin wire assumptions common to all wire moments formalisms. It is likely that the best choice of radius depends not only on the choice of integral equations, expansion functions, weighting functions, and methods of treating junctions, but also on the type of kernel approximations used in computing segment interactions and self terms. Consequently, guidelines should be investigated for each choice of formalism.

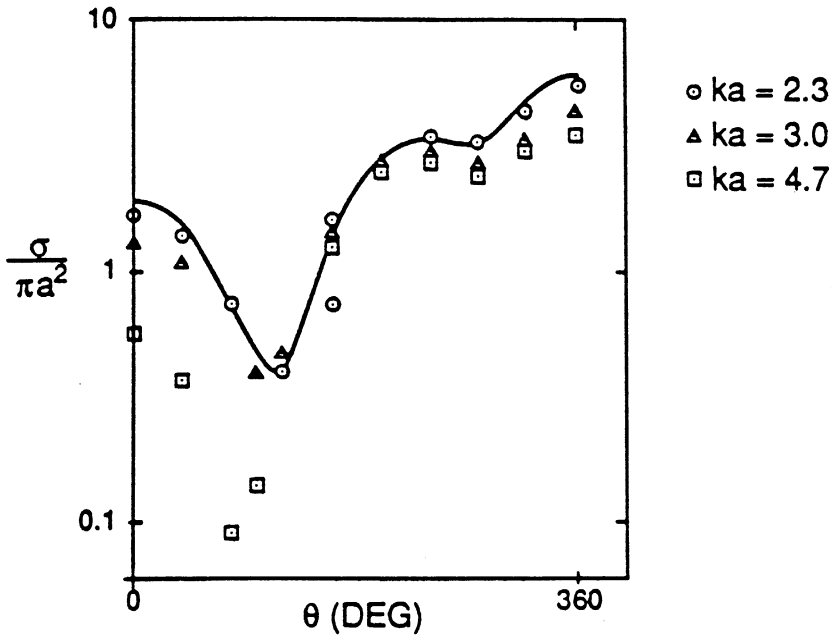

Figure 4. E-Plane Bistatic Scattering Cross Section For a Sphere with ka=2.3. (Line After King and Wu, Points From Model

7. CONVERSION TO SURFACE CURRENTS

Direct comparisons of shapes of wire grid current distributions and surface current distributions are possible in some cases. Surface current distributions for canonical problems are usually plotted as a function of one natural geometrical coordinate, with the current component either along or normal to the coordinate. If the wire segments in the grid lie along the natural coordinates and the grid is highly regular (mesh shapes repeated along the coordinate), excellent comparisons are possible.[1e,7] In such cases, the equivalent local component of the surface current density is approximately equal to the wire current divided by the distance between wires carrying the current. This fact is closely related to the assumptions inherent in wire grid modeling and in the thin wire moments formalism. It is assumed that the current is slowly varying over a region small compared to a wavelength. The wire current is assumed to be uniformly distributed around the wire. This information can be used to redistribute the grid currents on the modeled surface for grids of arbitrary shape.

Figure 5 shows a portion of a planar wire grid around the j-th surface subdomain, which has an area equal to A_j. This area is bounded by wire segments with lengths L_i which carry midpoint currents $\vec{I}_i$. The currents are complex and are spatial vectors. The magnitudes of the complex currents are spatial vectors denoted by $|\vec{I}_i|$. The surface subdomains bounding A_j and sharing common wire segments are shaded in Figure 5, and their areas are denoted by A_{ji} (not to be confused with matrix elements). The magnitude of the complex surface current density is a spatial vector denoted by $|\vec{J}_j|$. An approximate formula for this quantity is

$$|\vec{J}_j| = \sum_{\substack{i \\ \text{loop}}} \left(\frac{L_i}{A_j + A_{ji}} \right) |\vec{I}_i| \, . \tag{10}$$

The vector sum is over all segments bounding A_j . The coefficient in brackets is the reciprocal of an average width of the two areas joined by wire i, in the direction normal to the wire. For a square mesh, this formula reduces to the simple result mentioned earlier.

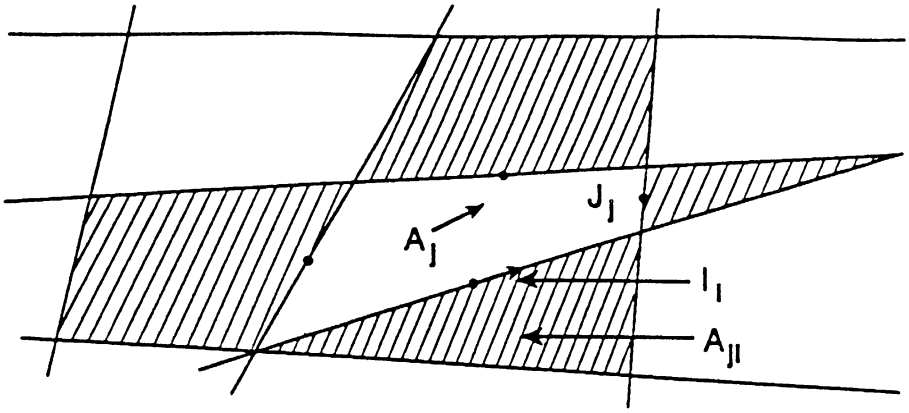

Figure 5. Equivalent Surface Currents From Wires

Several special cases must be considered. If one of the bounding wires is an edge wire, the corresponding value of A_{ji} is zero. The phases of all complex currents bounding A_j should be about the same.* The predicted surface current is the sum of currents from both sides of the modeled surface. If the surface is not closed, the predicted current cannot be uniquely separated into currents for each side. The formula gave reliable prediction for the sum of the two surface currents for example problems.

The formula was spot verified for square, rectangular, trapezoidal, and triangular mesh shapes in models of disks, spheres, and cylinders. For all meshes with four bounding wires, all wires were coplanar. For objects of arbitrary curvature, this may not always be possible. Slight deviations from planarity in a mesh should have little effect, and (10) should still be adequate. Large deviations result from poor modeling, since sharp bends should be modeled with wires along the bend.

---

* This should always be the case for regions small compared to a wavelength. The current phase and the interpretation of vector direction are interrelated, and are affected by the order in which segment ends are defined. It has been suggested[8] that the absolute value restrictions in (10) be removed. A paucity of surface current phase comparisons prevented verification of this suggestion.

The formula has not been verified for some special cases. For models with meshes in which an occasional surface subdomain was bounded by two nearly colinear segments, no local surface currents were available for comparison. The formula yields reasonably smooth current distributions in such regions and is presumed valid. For problems such as intersecting planes, some wires may border three or more surface areas. The formulas is not easily modified in this case, because one or more of the bordered areas may be in a shadow region with little current. For problems with symmetry in the geometry and excitation, wires normal to the expected direction of current flow are sometimes omitted even though the resulting mesh circumferences are greater than one wavelength. The formula is not appropriate for such models.

A more sophisticated formula could be generated using complicated interpolation methods. However, (10) is probably as accurate as is justified by wire grid modeling. If a poor model is used, no formula will give accurate surface currents.

8. SUMMARY AND PROSPECTUS

The banded matrix iterative method for solving linear simultaneous equations is useful for thin wire moments problems of intermediate electrical size. Compared to full matrix decomposition, the efficiency based on computer central processing time (or MOs) ranged from 35 for long, thin objects to about 10 for flat objects of significant width. Efficiencies of about 3 were found for fatter cylinders, and poor results were found for spheres. For flat objects, the guideline for bandwidth selection corresponding to about one-seventh of the object length resulted in reasonable convergence rates. Smaller bandwidths may be appropriate for long, thin objects. Larger bandwidths are required for short, fat objects. More examples might yield better guidelines. Even with use of the iterative method, the cost of solving large problems may be prohibitive for academic studies. Use of the method on machines of limited precision may lead to large rounding errors in the decomposition of the banded matrix. Partial pivoting may alleviate this problem, but at the expense of lower efficiency and increased storage requirements.

The computer program was recently converted to the CDC 7600 computer with no attempt at optimization for that machine. Up to 1250 unknowns have been used. Larger problems can be solved with minor code modifications. Optimization could greatly reduce the peripheral processor times, which currently dominate the dollar costs.

A limited study of wire grid modeling of surfaces established approximate guidelines for the specific moments formalism in use. The mesh circumference should not greatly exceed one-half wavelength. The segment length to wire radius ratio should be about 5 in regions of square mesh. Consistently good results were obtained, but no overall statement of accuracy was developed. The wire radius was constant for all segments in a single model, even though much smaller mesh sizes occurred near such regions as sphere poles. No deleterious effects of this practice were observed, which may indicate that further increases in wire radius would produce little change in currents.

The formula for converting grid currents to equivalent surface currents is useful for arbitrary mesh shapes. The accuracy of the computed surface currents is probably limited more by the accuracy of wire grid modeling than any other factor. The question concerning the phase of the predicted surface current should be investigated.

ADDENDUM

Since this work was originally performed, some additional insights into wire grid modeling have been developed. There follows a discussion of the wire length to radius ratios, wire grid models using regular polygons, and, finally, a different view of impedance matrices.

A.1 Wire Length/Radius Ratios

Conventional guidelines recommend that there be 10 wire segments per wavelength and that the wire segment length/radius ratio be 10 or greater. During investigations of the BMI solution technique, very good results were obtained with 5-6 wire segments per wavelength when the length/radius ratio was 5 to 6. This agreement held for both field values and surface current density when compared to analytical results.

While these were empirical results, their general validity has been substantiated in the open literature.[9,10] In these references, the EFIE MoM formalism is represented as:

$$(\underline{L}_o - \underline{L}) \bullet \underline{J} = - \underline{\ell} \bullet E_{inc}$$

where $\underline{L}_o$ is the usual electric field linear operator and $\underline{L}$ is a perturbation operator induced by representing a continuous surface by a wire grid. $\underline{L}$ is explicitly given by:

$$\underline{L} = jf\mu_o \, \underline{\ell} \bullet \ln\left(\frac{\ell}{2\pi r_o}\right)\left[\underline{I} - \frac{j\nabla\nabla}{k^2}\right]$$

where ℓ is the grid segment length, μ_o is the free space permeability ($4\pi 10^{-7}$), f is the frequency, k is the wave number, and r_o is the wire element radius. The perturbation term can be made to vanish using a length to radius ratio of 2π, which explains the empirical results obtained in the early GEMACS work of Ferguson and Balestri in which the ratio of 5 was used. Rewriting the segment length as a fraction of wavelength $\ell = \alpha\lambda$, the perturbation term $\underline{L}$ becomes:

$$\underline{L} = j\alpha 120\pi \ln\left(\frac{\ell}{2\pi r_o}\right)[\ldots]$$

which is recognizable as a fraction of the free space impedance of 377Ω. In the GEMACS, and also most other formulations, the self terms are dominated by the complex part of the interaction, and the terms are on the order of 10^3. We can that see the trade-off between the segment length and the length to radius ratio can alter the diagonal element of the structure matrix appreciably.

A.2 Wire Surface Grid Models

Another general rule is to attempt to have as much wire segment surface area as the actual surface being modeled. This rule has never been substantiated in the literature, however, there appears to be a conflict with the previous requirements. Consider a square mesh with each element having sides of length ℓ. If each wire element contributes 1/2 of its area to the interior (the other 1/2 contributes to the adjacent mesh) then we have:

$$\ell^2 = \tfrac{1}{2}[(8\pi r_o\ \ell\ )]$$

for the mesh area in terms of the wire segment parameters. This results in a length to radius ratio of 4π or approximately 10 which is where we started using the conventional modeling lore.

It would appear that the correct wire grid representations of surfaces lies somewhere in between, and the user should always make the ultimate decisions. It is natural to ask if there is a grid representation which supports a length to radius ratio of 2π and at the same time preserves the total surface area. In general the answer is no since there is no regular polygon for which this condition holds. The area of a regular polygon of n sides of length ℓ is:

$$A = \tfrac{1}{4} n\, \ell^2 \bullet \cot\left(\frac{\pi}{n}\right)$$

and the area of the n wire segments each of length ℓ is:

$$A_W = n \bullet 2\pi r_o\ \ell$$

Setting $A = \frac{1}{2} A_W$ leads to :

$$\cot\left(\frac{\pi}{n}\right) = \frac{4\pi r_o}{\ell}$$

or:

$$\frac{\ell}{r_o} = 4\pi\tan\left(\frac{\pi}{n}\right)$$

Setting n to 3, ..., 10 yields $\frac{\ell}{r_o}$ ratios and perturbation factors of:

n	$\frac{\ell}{r_o}$	$\ln\left(\frac{\ell}{2\pi r_o}\right)$
3	21.76	1.25
4	12.56	.69
5	9.13	.37
6	7.25	.14
7	6.05	-.04
8	5.20	-.18
9	4.57	-.31
10	4.08	-.43

for surface area modeling. It is seen that the $\frac{\ell}{r_o}$ ratio of 2π requires a seven-sided polygon, whereas the ratio of 4π requires 4-sided polygons which are typical planar surfaces. It is interesting to note that modeling surfaces with triangular meshes (n = 3) requires an extremely thin wire which will have a perturbation factor twice that of 4-sided polygons.

A.3 A Different View of Impedance Matrices

The banding scheme presented in the earlier work has since been referred to as the Principle Axis Slicing System or PASS. The problem with such a system is the fact that the interaction "strength" is assumed to be dependent on relative separation. It is possible for model elements to be quite far apart and still interact strongly to produce a scattered field when the elements are in phase. Figure A-3 is a magnitude plot of an impedance matrix. While there is a strong diagonal band, off band elements are clearly seen. Based on magnitude, a band-width can easily be selected as illustrated. Figure A-3 was originally displayed in color, and by using color graphics a different perspective of the "electromagnetics" of the model may

be obtained. Also, by assigning a reference phase, plotting the relative phases of the impedance matrix elements may indicate when certain regions of the model can interact coherently to produce large effects. I haven't attempted this since I think it will require more than the three colors available to me at present.

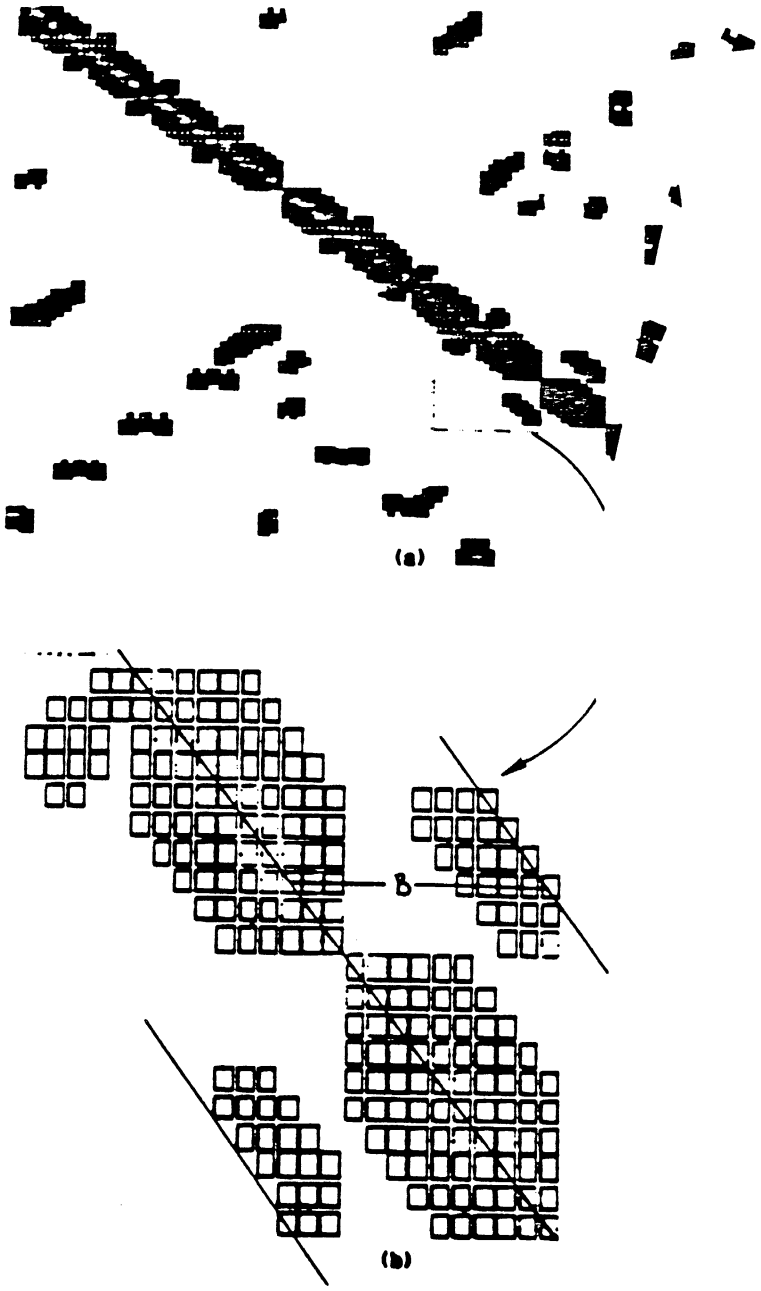

Figure A.3 (a,b) Impedance Matrix and Bandwidth Display

REFERENCES

1 Ferguson, T.R. The EMCAP (Electromagnetic Compatibility Analysis Program) Quarterly Reports, the BDM Corporation:

a. "Iterative Techniques in the Method-of-Moments," RADC-TR-75_121, May 1975

b. "Solution of Thin-Wire Moments Problems by Banded Matrix Iteration," RADC-TR-75-189, July 1975.

c. "Properties of the Banded Matrix Iterative Solution Technique for Thin-Wire Moments Problems," RADC-TR-75-272, November 1975.

d. "Wire Moments Problems of Intermediate Size," RADC-TR-76-148, February 1976.

e. "Wire Moments Problems of Large Size'" RADC-TR-76-122, May 1976.

2 Ferguson, T.R., Lehman, T.H., and Balestri, R.J. "Efficient Solutions of Large Moments Problems: Theory and Small Problems Results'" IEEE Trans. Ant. Prop., Vol. AP-24, March 1976.

3 The Antenna Modeling Program is a general purpose thin-wire code developed by MB Associates.

4 The GEMACS code, delivered to Mr. K. Siarkiewicz, Rome Air Development Center, Griffiss Air Force Base, New York 13440, under contract F30602-74-C-0182.

5 Karr, P. R. "Radiation Properties of Spherical Antennas as a Function of the Location of the Driving Force," J. Res. NBS, 46, No. 5, May 1951.

6 King, R.W.P. and Wu, T.T. The Scattering and Diffraction of Waves, Harvard University Press, Cambridge, 1959. Copyright 1959 by the President and Fellows of Harvard College.

7 Ferguson, T.R. and Balestri, R.J. "Solution of Large Wire Grid Moments Problems," IEEE International Symposium on Electromagnetic Compatibility, July 1976.

8 In conversation with Carl E. Baum

9 Kontorovich, N.I., "Averaged Boundary Conditions at the Surface of a Grating with Squaremesh," Rad. Eng. Electron, Phys., Vol 8, No. 9, 1963.

10 Lee, K.S.H., et al., "Limitations of Wire-Grid Modeling of a Closed Surface," IEEE-EMC-18, No. 3, Aug. 1976.